**Figure legends**

Figure 1. Muscle biopsy from Patient 1 taken at age 4 years.

(A) H&E stain shows marked variation in fiber size with neither fiber necrosis nor regeneration. (B) No nemaline bodies or cytoplasmic inclusions are revealed by mGT stain. On NADH-TR, intermyofibrillar networks are well organized. (D) On ATPase (pH 4.6), type 2A (A) and 2B (B) fibers are larger than type 1 (1) fibers. Bar=50 μm

Figure 2. Composition of mean muscle fiber diameter in each patient

(A) Mean diameters of type 1 fibers, (B) Mean diameters of type 2 fibers.

Filled squares represent LMNA-myopathy with FTD, open triangles show CFTD with *ACTA1* or *TPM3* mutations, and the solid line indicates the mean fiber diameter of age-matched controls for children at various ages taken from biopsies classified as normal. CFTD with *ACTA1* and *TPM3* mutations show type 1 fiber atrophy whereas LMNA-myopathy with FTD shows type 2 fiber hypertrophy.

Figure 3. Myonuclear shape changes in patient 2

Nuclear contours are irregular with a serpentine appearance. Bar=1μm

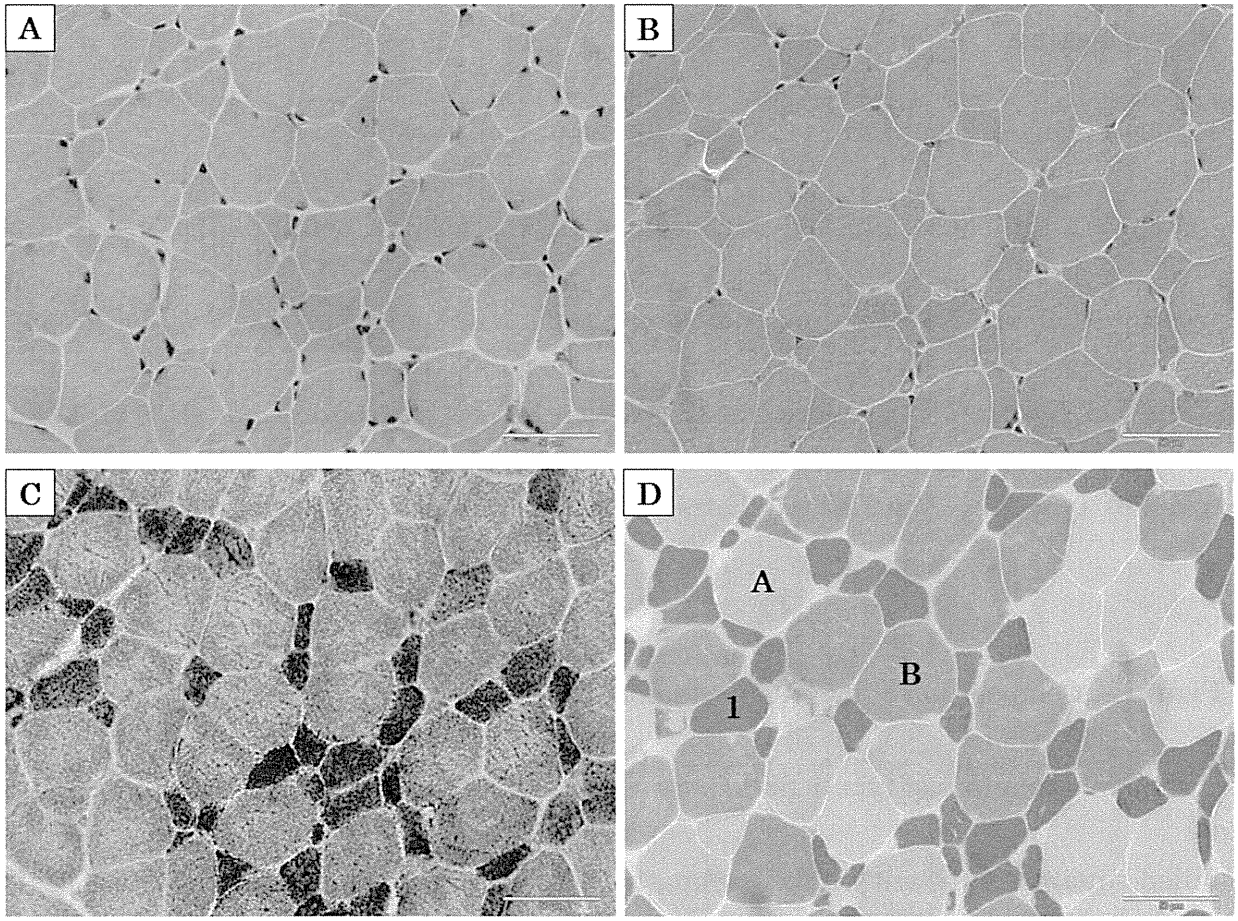


Figure 1

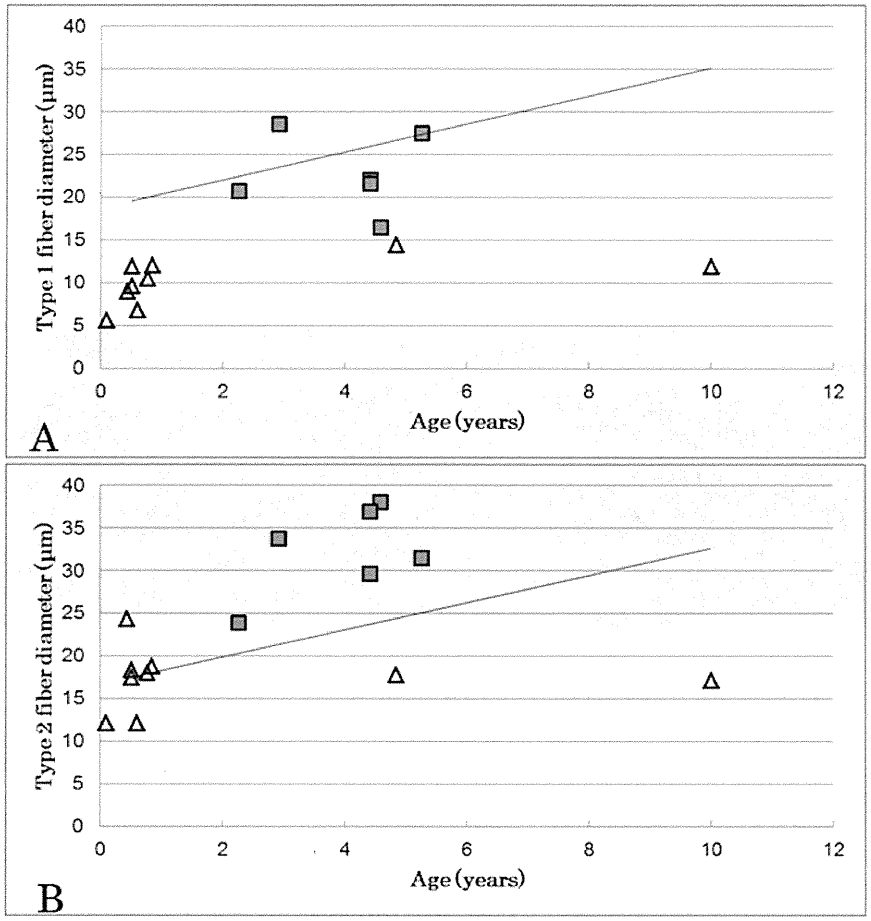


Figure 2

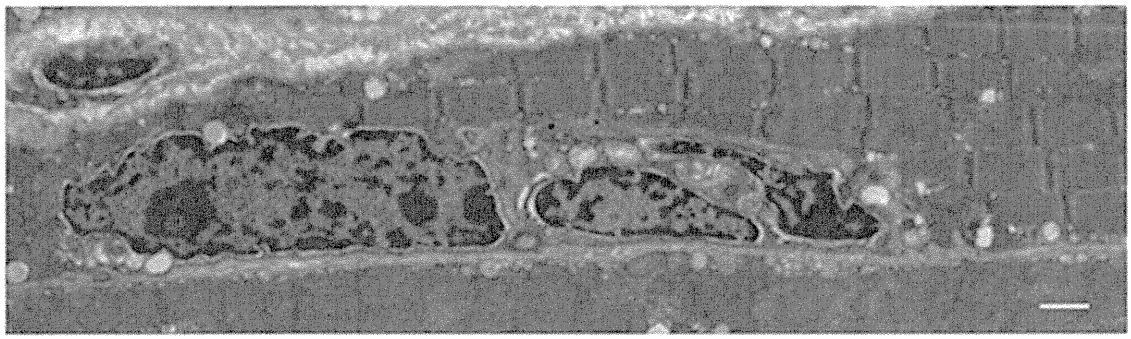

Figure 3

Table 1. Histological features of LMNA-myopathy patients with FTD, CFTD patients with *ACTA1* and *TPM3* mutations

| Patient No. | Muscle Biopsied | Age at Biopsy | Type 1 | | | Type 2A | | | Type 2B | | | Type 2C | %FSD | Mutation |
|---|---|---|---|---|---|---|---|---|---|---|---|---|---|---|
| | | | % | Mean Diameter (μM) | SD | % | Mean Diameter (μM) | SD | % | Mean Diameter (μM) | SD | | | |
| *LMNA* mutation | | | | | | | | | | | | | | |
| 1 | Biceps | 4y | 52 | 16.5 | 5.0 | 30 | 39.1 | 5.3 | 18 | 37.1 | 7.5 | 0 | 57 | c.367_369delAAG (p.K123del) |
| 2 | Quadriceps | 2y | 48 | 20.8 | 3.7 | 33 | 24.1 | 4.2 | 19 | 23.8 | 4.8 | 0 | 13 | c.99_101delGGA (p.E33del) |
| 3 | NA | 2y | 38 | 28.6 | 7.7 | 50 | 36.3 | 4.4 | 7 | 31.3 | 10.5 | 5 | 15 | c.1583C>A (p.T528K) |
| 4 | Biceps | 4y | 32 | 22.1 | 5.9 | 52 | 31.2 | 5.2 | 15 | 28.2 | 5.3 | 1 | 25 | c.1357C>T (p.R453W) |
| 5 | Biceps | 4y | 56 | 21.6 | 5.6 | 32 | 40.0 | 5.8 | 10 | 34.0 | 8.4 | 2 | 42 | c.1357C>T (p.R453W) |
| 6 | Biceps | 5y | 60 | 27.5 | 7.4 | 28 | 33.2 | 7.9 | 8 | 29.8 | 6.3 | 4 | 15 | c.907T>C (p.S303P) |
| *ACTA1* mutation | | | | | | | | | | | | | | |
| 1 | Biceps | 4y | 73 | 14.5 | 3.7 | 26 | 17.8 | 3.7 | 1 | — | — | 0 | 18 | c.16G>A (p.E6K) |

| | | | | | | | | | | | | | |
|---|---|---|---|---|---|---|---|---|---|---|---|---|---|
| 2 | Quadriceps | 0y6m | 60 | 11.9 | 3.1 | 10 | 18.0 | 2.8 | 20 | 18.8 | 2.8 | 10 | 35 | c.143G>T (p.G48C) |
| 3 | Quadriceps | 0y7m | 60 | 6.8 | 1.6 | 29 | 11.5 | 2.1 | 3 | — | — | 8 | 44 | c.143G>T (p.G48C) |
| 4 | NA | 0y1m | 52 | 5.6 | 1.5 | 28 | 14.4 | 2 | 12 | 10 | 2.8 | 8 | 57 | c.668T>C (p.L223P) |
| 5 | Biceps | 10y | 70 | 11.9 | 2.3 | 27 | 17.2 | 3.2 | 2 | — | — | 1 | 31 | c.682G>C (p.E228Q) |
| 6 | Biceps | 0y9m | 62 | 10.5 | 2.8 | 23 | 17.2 | 2.8 | 10 | 18.8 | 2.8 | 5 | 42 | c.981T>A (p.M326K) |
| 7 | Biceps | 0y10m | 72 | 12.0 | 1.8 | 22 | 19.5 | 3.5 | 3 | — | — | 3 | 36 | c.1000C>T (p.P332S) |
| *TPM3* mutation | | | | | | | | | | | | | | |
| 1 | Biceps | 0y5m | 56 | 9.0 | 2.4 | 44 | 24.4 | 3.2 | 0 | — | — | 0 | 63 | c.502C<T (p.R168C) |
| 2 | Biceps | 0y6m | 58 | 9.7 | 2.0 | 20 | 17.9 | 2.5 | 16 | 17.1 | 2.4 | 6 | 45 | c.502C<T (p.R168C) |

SD = standard deviation; NA = data not available; dash = not applicable

Table 2. Clinical and pathological summary of LMNA-myopathy patients with FTD

| Patient No | Sex | Age at Diagnosis (yr) | Age at biopsy (yr) | Pathological diagnose | Age at walk (mo) | Hypotonia | High arched palate | Respiratory involvement | Cardiac symptoms | Other presenting signs/ Symptoms (age/yr) | CK (IU/L) | FSD (%) |
|---|---|---|---|---|---|---|---|---|---|---|---|---|
| 1 | M | 16 | 4 | CFTD | 12 | Yes | No | No | AV-b, ICRBBB (16yr) | Joint contractures (4) | 330 | 57 |
| 2 | M | 4 | 2 | CFTD | 14 | Yes | No | No | No | Joint contractures (2) Dropped head (4) Rigid spine (4) | 367 | 13 |
| 3 | M | 10 | 2 | MD | 15 | Yes | No | No | No | Joint contractures (2) Rigid spine (8) | 1098 | 15 |

| | | | | | | | | | | | | |
|---|---|---|---|---|---|---|---|---|---|---|---|---|
| 4 | F | 4 | 4 | MD | 12 | Yes | No | No | No | No | 1408 | 25 |
| 5 | F | 13 | 4 | MD | 14 | No | No | No | No | Lordosis (4)<br>Joint contracture (6)<br>Rigid spine (10) | 1985 | 42 |
| 6 | F | 5 | 5 | MD | 18 | No | No | No | No | No | 303 | 15 |

MD; muscular dystrophy, AV-b; atrioventricular block, IRBBB; incomplete right bundle-branch block, PAF; paroxysmal atrial fibrillation

Patients 1 and 2 were initially diagnosed as having CFTD. Patients 3 to 7 were genetically confirmed to have LMNA-myopathy with FTD. None of the patients had a high arched palate and/or respiratory involvement. Serum creatine kinase (CK) was mildly elevated in all patients

Table 3. Comparison of clinical and pathological information between LMNA-myopathy with FTD and CFTD with *ACTA1* and *TPM3* mutations

| Gene mutation | *LMNA* | *ACTA1* | *TPM3* |
|---|---|---|---|
| Number of patients | 6 | 7 | 2 |
| Onset | Infantile | at birth | < 2months |
| Hypotonia | 67% (4/6) | 100% (7/7) | 100% (2/2) |
| High arched palate | 0% (0/6) | 57% (4/7) | 50% (1/2) |
| Respiratory involvement | 0% (0/6) | 57% (4/7) | 0% (0/2) |
| Joint contracture | 67% (4/6) | 14% (1/7) | 0% (0/2) |
| CK level (IU/L) | 963±662 | 53±15 | 42±16 |
| Type 1 fiber predominance | 33% (2/6) | 86% (6/7) | 100% (2/2) |
| Type 2B fiber deficiency | 0% (0/6) | 57% (4/7) | 50% (1/2) |

Type 1 fiber predominance and absence of type 2B fibers were common in CFTD caused by *ACTA1* or *TMP3* mutations. Type 2B fiber deficiency was not seen in LMNA-myopathy with FTD. Serum creatine kinase (CK) levels were significantly higher in LMNA-myopathy than in CFTD with *ACTA1* and *TPM3* mutations ($p < 0.05$).

Highlights

- *LMNA* mutation was found in congenital fiber type disproportion (CFTD) patients.
- Fiber type disproportion is often seen in *LMNA*-related muscular dystrophy.
- Fiber type disproportion in LMNA-myopathy is due to hypertrophy of fast fibers.
- LMNA-myopathy should be considered whenever a diagnosis of CFTD is made.

JNNP Online First, published on September 11, 2013 as 10.1136/jnnp-2013-305587


RESEARCH PAPER

# Mutation profile of the *GNE* gene in Japanese patients with distal myopathy with rimmed vacuoles (GNE myopathy)

Anna Cho,[1] Yukiko K Hayashi,[1,2,3] Kazunari Monma,[1] Yasushi Oya,[4] Satoru Noguchi,[1] Ikuya Nonaka,[1] Ichizo Nishino[1,2]

► Additional material is published online only. To view please visit the journal online (http://dx.doi.org/10.1136/jnnp-2013-305587).

[1]Department of Neuromuscular Research, National Institute of Neuroscience, National Center of Neurology and Psychiatry, Tokyo, Japan
[2]Department of Clinical Development, Translational Medical Center, National Center of Neurology and Psychiatry, Tokyo, Japan
[3]Department of Neurophysiology, Tokyo Medical University, Tokyo, Japan
[4]Department of Neurology, National Center Hospital, National Center of Neurology and Psychiatry, Tokyo, Japan

**Correspondence to**
Professor Yukiko K Hayashi, Department of Neurophysiology, Tokyo Medical University, 6-1-1 Shinjuku, Shinjuku, Tokyo 160-8402, Japan; yhayashi@tokyo-med.ac.jp

Received 4 June 2013
Revised 21 August 2013
Accepted 22 August 2013

**To cite:** Cho A, Hayashi YK, Monma K, *et al. J Neurol Neurosurg Psychiatry* Published Online First: [*please include* Day Month Year] doi:10.1136/jnnp-2013-305587

## ABSTRACT

**Background** GNE myopathy (also called distal myopathy with rimmed vacuoles or hereditary inclusion body myopathy) is an autosomal recessive myopathy characterised by skeletal muscle atrophy and weakness that preferentially involve the distal muscles. It is caused by mutations in the gene encoding a key enzyme in sialic acid biosynthesis, UDP-*N*-acetylglucosamine 2-epimerase/*N*-acetylmannosamine kinase (GNE).

**Methods** We analysed the *GNE* gene in 212 Japanese GNE myopathy patients. A retrospective medical record review was carried out to explore genotype–phenotype correlation.

**Results** Sixty-three different mutations including 25 novel mutations were identified: 50 missense mutations, 2 nonsense mutations, 1 insertion, 4 deletions, 5 intronic mutations and 1 single exon deletion. The most frequent mutation in the Japanese population is c.1714G>C (p.Val572Leu), which accounts for 48.3% of total alleles. Homozygosity for this mutation results in more severe phenotypes with earlier onset and faster progression of the disease. In contrast, the second most common mutation, c.527A>T (p.Asp176Val), seems to be a mild mutation as the onset of the disease is much later in the compound heterozygotes with this mutation and c.1714G>C than the patients homozygous for c.1714G>C. Although the allele frequency is 22.4%, there are only three homozygotes for c.527A>T, raising a possibility that a significant number of c.527A>T homozygotes may not develop an apparent disease.

**Conclusions** Here, we report the mutation profile of the *GNE* gene in 212 Japanese GNE myopathy patients, which is the largest single-ethnic cohort for this ultra-orphan disease. We confirmed the clinical difference between mutation groups. However, we should note that the statistical summary cannot predict clinical course of every patient.

## INTRODUCTION

GNE myopathy, which is also known as distal myopathy with rimmed vacuoles,[1] quadriceps sparing myopathy[2] or hereditary inclusion body myopathy (hIBM),[3] is an autosomal recessive myopathy characterised by skeletal muscle atrophy and weakness that preferentially involve the distal muscles such as the tibialis anterior. It is a progressive disease, whereby the symptoms of muscle weakness start to affect the patient from the second or third decade of life, and most of the patients become wheelchair-bound between twenties and sixties.[4] The characteristic histopathological features in muscle biopsy include muscle fibre atrophy with the presence of rimmed vacuoles and intracellular congophilic deposits.[4 5] GNE myopathy is caused by mutations in the gene encoding a key enzyme in sialic acid biosynthesis, UDP-*N*-acetylglucosamine 2-epimerase/*N*-acetylmannosamine kinase (GNE).[6–8] Genetically confirmed GNE myopathy was initially recognised in Iranian Jews and Japanese,[7 9] but later appeared to be widely distributed throughout the world. More than 100 mutations in the *GNE* gene have been described up to date.

During the last decade, there has been extensive experimental work to elucidate the pathogenesis and to develop therapeutic strategies of GNE myopathy.[6 10–12] Better knowledge on the basis of those research achievements have currently enabled us to enter the era of clinical trial for human patients. At this moment, the identification of new GNE myopathy patients with precise genetic diagnosis and the expansion of global spectrum of *GNE* mutations are timely and important. Here, we report the molecular profile of Japanese GNE myopathy patients with a brief discussion of genotype–phenotype correlations.

## METHODS

### Patients

Two hundred and twelve patients from 201 unrelated Japanese families were included in this study. There were 117 female and 95 male patients. All cases were genetically confirmed as GNE myopathy. A retrospective medical record review was carried out to explore genotype–phenotype correlation. Informed consent was obtained for the collection of clinical data and extraction of DNA to perform mutation analysis.

### Genetic analysis

DNA was extracted from peripheral blood leukocytes or skeletal muscle tissue. We used the previously described sequencing method to describe mutations at cDNA level.[7] All exons and splice regions of the *GNE* gene were sequenced. NM_005476.5 was used as a reference sequence. We screened 100 alleles from normal Japanese individuals to determine the significance of novel variations.

### Pathological analysis

To evaluate histopathological phenotype according to genotype, we analysed muscle biopsies from two

most common genotype groups in Japanese population. Each of the three age-matched and biopsy site-matched samples from c.1714G>C homozygous group and c.1714G>C/c.527A>T compound heterozygous group was compared. Muscle samples were taken from biceps brachii and frozen with isopentane cooled in liquid nitrogen. Serial frozen sections of 10 μm were stained using a set of histochemical methods including haematoxylin-eosin and modified Gomori trichrome.

### Statistical analysis

Statistics were calculated using GraphPad Prism 5 software (GraphPad Software, La Jolla, California, USA). Between-group comparison for clinical data was performed using one-way analysis of variance with Dunnett's post-test. All values are expressed as means±SD. We performed two-sided tests with a $p<0.05$ level of significance.

## RESULTS

### Mutation profile

We identified homozygous or compound heterozygous *GNE* mutations in all 212 patients (see online supplement 1). In total, 63 different mutations were found including 50 missense mutations, 2 nonsense mutations, 1 insertion, 4 deletions, 5 intronic mutations and 1 single exon deletion (figure 1). Twenty-five novel mutations were identified including 17 missense mutations, 4 small deletions, 3 intronic mutations and 1 single exon deletion (figure 1, see online supplement).

Twenty-one mutations were found to be shared between two or more unrelated families. The three mutations occurring most frequently in the Japanese population were c.1714G>C (p.Val572Leu), c.527A>T (p.Asp176Val) and c.38G>C (p.Cys13Ser); these comprised 48.3%, 22.4% and 3.5%, respectively, of the total number of alleles examined (table 1).

Table 1 Allele frequency for GNE mutations in 212 Japanese GNE myopathy patients

| | Allele frequency |
|---|---|
| Mutation type | |
| Missense | 402 (94.8%) |
| Nonsense | 3 (0.7%) |
| Insertion | 1 (0.2%) |
| Small deletion | 4 (0.9%) |
| Single exon deletion | 2 (0.5%) |
| Intron | 12 (2.8%) |
| Three most common mutations | |
| c.1765G>C (p.Val572Leu) | 205 (48.3%) |
| c.578A>T (p.Asp176Val) | 95 (22.4%) |
| c.38G>C (p.Cys13Ser) | 15 (3.5%) |
| Total alleles | 424 |

### Genotype–phenotype correlations

The mean age of genetic analysis was 41.6±14.1 years (n=212), and the mean age of symptom onset based on the data available was 28.4±10.2 years (n=195). The earliest onset age was 10 and the latest was 61 years old in our cohort. Thirty-six among 154 patients (23.4%) were full-time wheelchair users at the point of genetic diagnosis with the average age at loss of ambulation being 36.8±11.3 years (n=36). The youngest wheelchair-bound age was 19, and the oldest ambulant age was 78. To investigate genotype–phenotype correlations in the major *GNE* mutations of Japanese population, we compared the age at symptom onset and loss of ambulation between the patients groups carrying either of the two most frequent mutations, c.1714G>C and c.527A>T (table 2). As with a previous report,[13] homozygous c.1714G>C mutations resulted in earlier symptom onset (23.9±7.1 years, $p<0.01$) and the majority of full-time wheelchair users were in this group. On the other hand, c.1714G>C/c.527A>T compound heterozygous patients first developed symptoms at a later age (37.6±12.6 years, $p<0.01$), and there were no wheelchair-bound patients at the time of genetic analysis in this group. Only three homozygous c.527A>T mutation patients were identified, and their average onset age (32.3±5.7 years) was also higher among total patients (28.4±10.2 years). All three patients were ambulant until the last follow-up visits (29, 40 and 44 years).

Among 212 cases, 80 patients underwent muscle biopsies. Overall pathological findings in our series were compatible with GNE myopathy. The characteristic rimmed vacuoles were observed in the majority (76/80, 95.0%) of the cases. Through the analysis of muscle biopsies from age-matched and biopsy site-matched samples, we found that the histopathological phenotypes were in line with these genotype–phenotype correlations (figure 2). Homozygous c.1714G>C mutations have led to much more advanced pathological changes with severe myofibre atrophy and increased numbers of rimmed vacuoles. Marked adipose tissue replacement was appreciated in a case with reflecting very advanced stage of muscle degeneration.

## DISCUSSION

As shown in figure 1, mutations were located throughout the whole open reading frame of the *GNE* gene. The majority (94.8%, 402/424 alleles) of the mutations in our series were missense mutations (table 1), and there were no homozygous null mutations. These results are in accordance with previous reports[7 9] signifying that total loss of GNE function might be

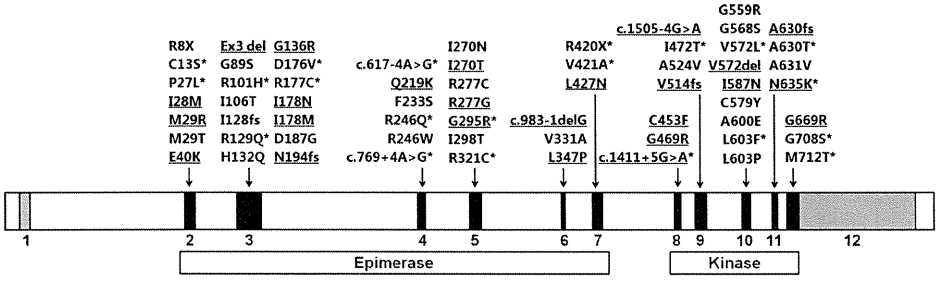


Figure 1 Mutation spectrum of *GNE* in the Japanese population. The mutations are located throughout the whole open reading frame. Twenty-five novel mutations are underlined, and 21 shared mutations are indicated with asterisks.

Table 2 Comparison of clinical course between two most frequent GNE mutations in Japanese population

| Mutations | Age at exam (years) | | Age at onset (years) | | Age at WB (years) | | Ambulant |
|---|---|---|---|---|---|---|---|
| c.1714G>C/c.1714G>C | 38.6±13.4 | (n=71) | 23.9±7.1 | (n=65)** | 35.4±10.6 | (n=28) | n=22 |
| c.1714G>C/other | 32.3±13.2 | (n=25) | 21.9±6.8 | (n=22)* | 37.0±8.6 | (n=4) | n=16 |
| c.1714G>C/c.527A>T | 48.9±14.1 | (n=38) | 37.6±12.6 | (n=35)** | | (n=0) | n=29 |
| c.527A>T/c.527A>T | 37.7±7.7 | (n=3) | 32.3±5.7 | (n=3) | | (n=0) | n=3 |
| c.527A>T/other | 41.3±11.1 | (n=51) | 30.6±8.0 | (n=46) | | (n=2) | n=33 |
| other/other | 49.8±14.7 | (n=24) | 28.8±9.5 | (n=24) | | (n=2) | n=16 |
| Total | 41.6±14.1 | (n=212) | 28.4±10.2 | (n=195) | 36.8±11.3 | (n=36) | n=118 |

Dunnett's multiple comparison test (control: total patients) *p<0.05, **p<0.01.
Other: a mutation other than c.1714G>C and c.527A>T; WB, wheelchair-bound.

lethal in human beings. The embryonic lethality of null mutation in *GNE* had also been proved in the mouse model.[14] Only three of total 212 patients carried a nonsense mutation; clinical data were available for two of them. Interestingly, one patient with compound heterozygous c.22C>T (p.Arg8X)/c.1714G>C (p.Val572Leu) mutations developed his first symptoms at the age of 15, while the other patient with c.1258C>T (p.Arg420X)/c.527A>T (p.Asp176Val) mutations developed her symptoms much later, at the age of 45. The similar difference was also observed in the phenotypes of patients with frame-shift mutations. A patient carrying c.383insT (p.I128fs) and c.1714G>C (p.Val572Leu) mutations developed his first symptom at the age of 13, whereas another two patients with c.1541-4del4 (p.Val514fs)/c.527A>T (p.Asp176Val) and c.581delA (p.N194fs)/c.527A>T (p.Asp176Val) mutations had later symptom onset, at the age of 30 and 32 years, respectively. This clinical variation can be explained as it reflects alternative missense mutations, because the two patients with very early onset shared the same missense mutation c.1714G>C, while the patients with the milder phenotype shared c.527A>T.

Among five intronic mutations identified in our series, c.617 −4A>G and c.769 + 4A>G were previously reported as pathological mutations.[7 15] Three novel variants were located at splice junction of exon 6 (c.983–1delG), exon 8 (c.1411 +5G>A) and exon 9 (c.1505–4G>A), raising the high possibility of relevant exons skipping. These variants were not detected in 200 alleles from normal Japanese individuals and also in the single nucleotide polymorphism (SNP) database.

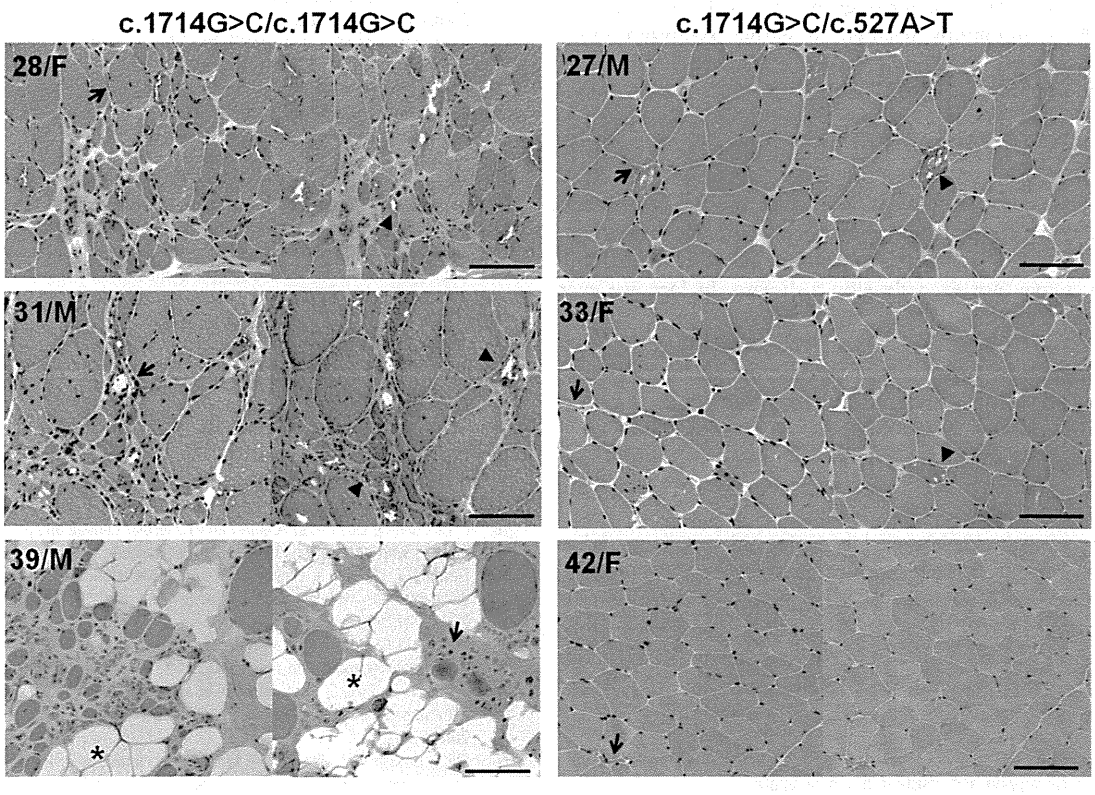


Figure 2 Comparison of muscle pathology between patients with homozygous c.1714G>C (p.Val572Leu) and with compound heterozygous c.1714G>C (p.Val572Leu)/c.527A>T (p.Asp176Val) mutations. Homozygous c.1714G>C (p.Val572Leu) mutations have led to much more advanced histopathological changes compared with compound heterozygous c.1714G>C (p.Val572Leu)/c.527A>T (p.Asp176Val) mutations. Haematoxylin-eosin (left) and modified Gomori trichrome (right) stains of muscle sections from age (c.1714G>C/c.1714G>C: 28, 31 and 39 years, c.1714G>C/c.527A>T: 27, 33 and 42 years) and biopsy site (biceps brachii muscles) matched samples. Bar=100μm; triangles: rimmed vacuoles; arrows: atrophic fibres; asterisks: adipose tissue.

As there are ethnic differences in *GNE* mutation frequencies,[9 16–19] establishing the mutation spectrum and defining predominant mutations in a certain population may be helpful for the diagnosis. Three most common mutations in the Japanese population and their allele frequencies (table 1) were in agreement with previous data.[7 13] The allele frequencies of top two mutations (c.1714G>C and c.527A>T) comprise more than two-third of the total number of alleles suggesting that founder effects are involved in the relatively higher incidence of GNE myopathy in Japan.

Although most of patients showed characteristic pathological features, the existence of exceptional cases with atypical biopsy findings implies that GNE myopathy cannot be totally excluded from the absence of rimmed vacuoles in muscle biopsies. On the other hand, we found 94 patients who were pathologically or clinically suspected but not had mutations in *GNE*. Several cases of VCP myopathy mutations in (*VCP*), myofibrillar myopathy mutations in (*DES*) and reducing body myopathy (*FHL1*) were later identified in this group, suggesting these diseases should be included as differential diagnosis of GNE myopathy.[20]

In terms of genotype–phenotype correlations, we confirmed that homozygosity for c.1714G>C (p.Val572Leu) mutation resulted in more severe phenotypes in clinical and histopathological aspects. In contrast, the second most common mutation, c.527A>T (p.Asp176Val), seems to be a mild mutation as the onset of the disease is much later in the compound heterozygotes with this mutation and c.1714G>C. Several evidences further strengthened the link between the more severe phenotype and c.1714G>C, and between the milder phenotype and c.527A>T. Compound heterozygosity for c.1714G>C and non-c.527A>T mutations resulted in earlier symptom onset (22.9±6.8 years, $p<0.05$) compared with the average onset age of the total group, whereas c.527A>T, both presented as homozygous and as compound heterozygous mutations, lead to slower disease progression (table 2). In addition, only three patients carrying this second most common mutation c.527A>T in homozygous mode were identified, which is much fewer than the number expected from high allele frequency (22.4%), raising a possibility that considerable number of c.527A>T homozygotes may not even develop a disease. In fact, we ever identified an asymptomatic c.527A>T homozygote at age 60 years.[7] Now he is at age 71 years and still healthy. Overall, these results indicate that different mutations lead to different spectra of severity. However, this is a result of a statistical summary that cannot predict clinical course of each individual patient.

Here, we presented the molecular bases of 212 Japanese GNE myopathy patients with 25 novel *GNE* mutations. Based on the current status of knowledge, sialic acid supplementation may lead to considerable changes in the natural course of GNE myopathy within near future. The ongoing identification of *GNE* mutations and further studies regarding the clinicopathological features of each mutation will provide better understanding of GNE myopathy and lead to accelerated development of treatment for this disease.

**Acknowledgements** The authors thank Kanako Goto and Yuriko Kure for their invaluable technical support and assistant in genetic analysis.

**Contributors** AC had full access to all of the data in the study and wrote the manuscript; YKH supervised all aspects of this study including study design, data interpretation and manuscript preparation; KM and YO participated in collecting and analysing all the clinical and genetic data; SN, I Nonaka and I Nishino were involved in data analysis and interpretation and also supervised manuscript preparation.

**Funding** This study was supported partly by Intramural Research Grant 23-4, 23-5, 22-5 for Neurological and Psychiatric Disorders of NCNP; partly by Research on Intractable Diseases, Comprehensive Research on Disability Health and Welfare, and Applying Health Technology from the Ministry of Health Labour and Welfare; and partly by JSPS KAKENHI Grant Number of 23390236.

**Competing interests** None.

**Ethics approval** This study was approved by the ethics committee of National Center of Neurology and Psychiatry.

**Provenance and peer review** Not commissioned; externally peer reviewed.

## REFERENCES

1 Nonaka I, Sunohara N, Ishiura S, *et al*. Familial distal myopathy with rimmed vacuole and lamellar (myeloid) body formation. *J Neurol Sci* 1981;51:141–55.
2 Argov Z, Yarom R. "Rimmed vacuole myopathy" sparing the quadriceps. A unique disorder in Iranian Jews. *J Neurol Sci* 1984;64:33–43.
3 Askanas V, Engel WK. New advances in the understanding of sporadic inclusion-body myositis and hereditary inclusion-body myopathies. *Curr Opin Rheumatol* 1995;7:486–96.
4 Nonaka I, Noguchi S, Nishino I. Distal myopathy with rimmed vacuoles and hereditary inclusion body myopathy. *Curr Neurol Neurosci Rep* 2005;5:61–5.
5 Nishino I, Malicdan MC, Murayama K, *et al*. Molecular pathomechanism of distal myopathy with rimmed vacuoles. *Acta Myol* 2005;24:80–3.
6 Eisenberg I, Avidan N, Potikha T, *et al*. The UDP-N-acetylglucosamine 2-epimerase/N-acetylmannosamine kinase gene is mutated in recessive hereditary inclusion body myopathy. *Nat Genet* 2001;29:83–7.
7 Nishino I, Noguchi S, Murayama K, *et al*. Distal myopathy with rimmed vacuoles is allelic to hereditary inclusion body myopathy. *Neurology* 2002;59:1689–93.
8 Keppler OT, Hinderlich S, Langner J, *et al*. UDP-GlcNAc 2-epimerase: a regulator of cell surface sialylation. *Science* 1999;284:1372–6.
9 Eisenberg I, Grabov-Nardini G, Hochner H, *et al*. Mutations spectrum of *GNE* in hereditary inclusion body myopathy sparing the quadriceps. *Hum Mutat* 2003;21:99.
10 Noguchi S, Keira Y, Murayama K, *et al*. Reduction of UDP-N-acetylglucosamine 2-epimerase/N-acetylmannosamine kinase activity and sialylation in distal myopathy with rimmed vacuoles. *J Biol Chem* 2004;279:11402–7.
11 Malicdan MC, Noguchi S, Nonaka I, *et al*. A Gne knockout mouse expressing human *GNE* D176V mutation develops features similar to distal myopathy with rimmed vacuoles or hereditary inclusion body myopathy. *Hum Mol Genet* 2007;16:2669–82.
12 Malicdan MC, Noguchi S, Hayashi YK, *et al*. Prophylactic treatment with sialic acid metabolites precludes the development of the myopathic phenotype in the DMRV-hIBM mouse model. *Nat Med* 2009;15:690–5.
13 Mori-Yoshimura M, Monma K, Suzuki N, *et al*. Heterozygous UDP-GlcNAc 2-epimerase and N-acetylmannosamine kinase domain mutations in the *GNE* gene result in a less severe GNE myopathy phenotype compared to homozygous N-acetylmannosamine kinase domain mutations. *J Neurol Sci* 2012;318:100–5.
14 Schwarzkopf M, Knobeloch KP, Rohde E, *et al*. Sialylation is essential for early development in mice. *Proc Natl Acad Sci USA* 2002;99:5267–70.
15 Ikeda-Sakai Y, Manabe Y, Fujii D, *et al*. Novel Mutations of the *GNE* gene in distal myopathy with rimmed vacuoles presenting with very slow progression. *Case Rep Neurol* 2012;4:120–5.
16 Li H, Chen Q, Liu F, *et al*. Clinical and molecular genetic analysis in Chinese patients with distal myopathy with rimmed vacuoles. *J Hum Genet* 2011;56:335–8.
17 Liewluck T, Pho-Iam T, Limwongse C, *et al*. Mutation analysis of the *GNE* gene in distal myopathy with rimmed vacuoles (DMRV) patients in Thailand. *Muscle Nerve* 2006;34:775–8.
18 Kim BJ, Ki CS, Kim JW, *et al*. Mutation analysis of the *GNE* gene in Korean patients with distal myopathy with rimmed vacuoles. *J Hum Genet* 2006;51:137–40.
19 Broccolini A, Ricci E, Cassandrini D, *et al*. Novel *GNE* mutations in Italian families with autosomal recessive hereditary inclusion-body myopathy. *Hum Mutat* 2004;23:632.
20 Shi Z, Hayashi YK, Mitsuhashi S, *et al*. Characterization of the Asian myopathy patients with VCP mutations. *Eur J Neurol* 2012;19:501–9.

# Mutation profile of the *GNE* gene in Japanese patients with distal myopathy with rimmed vacuoles (GNE myopathy)

Anna Cho, Yukiko K Hayashi, Kazunari Monma, et al.

*J Neurol Neurosurg Psychiatry* published online September 11, 2013
doi: 10.1136/jnnp-2013-305587

**Notes**

Available online at www.sciencedirect.com

SciVerse ScienceDirect

Neuromuscular Disorders xxx (2013) xxx–xxx

www.elsevier.com/locate/nmd

Case report

# Fatal hepatic hemorrhage by peliosis hepatis in X-linked myotubular myopathy: A case report

T. Motoki [a,*], M. Fukuda [d], T. Nakano [a], S. Matsukage [b], A. Fukui [c], S. Akiyoshi [e], Y.K. Hayashi [f,g], E. Ishii [d], I. Nishino [f,g]

[a] *Department of Pediatrics, Uwajima City Hospital, Uwajima, Ehime, Japan*
[b] *Pathology, Uwajima City Hospital, Uwajima, Ehime, Japan*
[c] *Radiology, Uwajima City Hospital, Uwajima, Ehime, Japan*
[d] *Department of Pediatrics, Ehime University Graduate School of Medicine, Toon, Ehime, Japan*
[e] *Department of Neonatology, Ehime Prefectural Central Hospital, Matsuyama, Ehime, Japan*
[f] *Department of Neuromuscular Research, National Institute of Neuroscience, National Center of Neurology and Psychiatry (NCNP), Tokyo, Japan*
[g] *Department of Clinical Development, Translational Medical Center, NCNP, Kodaira, Tokyo, Japan*

Received 31 October 2012; received in revised form 4 May 2013; accepted 11 June 2013

**Abstract**

We report a 5-year-old boy with X-linked myotubular myopathy complicated by peliosis hepatis. At birth, he was affected with marked generalized muscle hypotonia and weakness, which required permanent ventilatory support, and was bedridden for life. He died of acute fatal hepatic hemorrhage after using a mechanical in-exsufflator. Peliosis hepatis, defined as multiple, variable-sized, cystic blood-filled spaces through the liver parenchyma, was confirmed by autopsy. To avoid fatal hepatic hemorrhage by peliosis hepatis, routine hepatic function tests and abdominal imaging tests should be performed for patients with X-linked myotubular myopathy, especially at the time of using artificial respiration.


*Keywords:* X-linked myotubular myopathy; Hepatic hemorrhage; Peliosis hepatis; Mechanical in-exsufflator

## 1. Introduction

X-linked myotubular myopathy (XLMTM) is one of the most serious types of centronuclear ("myotubular") myopathies, which is pathologically characterized by a high proportion of small myofibers with centrally placed nuclei [1]. With recent advances in molecular analysis, centronuclear myopathy has been classified into three genetic subtypes. XLMTM is a severe form of centronuclear myopathy presenting with symptoms from birth, including respiratory failure, ophthalmoplegia, and muscle weakness [2]. XLMTM is caused by genetic aberration of the *MTM1* gene on chromosome Xq28 [3]. *MTM1* encodes myotubularin, a dual-specificity 3-phosphoinositide phosphatase, which plays an important role in the regulation of signaling pathways involved in muscle growth and differentiation [3].

Although XLMTM is considered to be a fatal disorder within the first year of life, it has been recently shown that more than half of XLMTM patients achieve prolonged survival, and most of the long-term survivors suffer from several complications in several organ systems [4]. Among them, peliosis hepatis is a rare condition that can affect children and cause fatal hepatic hemorrhage. A few reports have suggested that XLMTM patients might be at risk for development of peliosis hepatis [4–7]. We report a 5-year-old patient with XLMTM who suffered

* Corresponding author. Address: Department of Pediatrics, Uwajima City Hospital, 1-1 Goten-cho, Uwajima, Ehime 798-8510, Japan. Tel.: +81 895 25 1111; fax: +81 895 25 5334.
*E-mail address:* tmotoki@m.ehime-u.ac.jp (T. Motoki).

0960-8966/$ - see front matter © 2013 Elsevier B.V. All rights reserved.
http://dx.doi.org/10.1016/j.nmd.2013.06.008

from fatal peliosis hepatis. In addition, the clinical features and prevention approach of fatal hepatic hemorrhage in XLMTM are also discussed.

## 2. Case report

A full-term male was born at 39 weeks of gestational age by normal spontaneous vaginal delivery and weighed 2728 g. The Apgar score was 5 at 1 min and 7 at 5 min. There was no abnormal antenatal symptom (e.g. polyhydramnios, reduced fetal movements, and thinning of the ribs). And neither family history of genetic disorders nor medical problem during perinatal period was observed. At birth, however, marked generalized muscle hypotonia and weakness, which required ventilatory support, appeared in the patient. On physical examination, facial muscle weakness and a high-arched palate were detected, and extraocular muscle involvement was not detected. The hypotonia did not improve with conventional management. The karyotype of peripheral blood was normal. A muscle biopsy from the biceps branch was performed under the possible diagnosis of neuromuscular disease. All muscle fibers were small and round (Fig. 1a), and a peripheral halo was observed in most fibers (Fig. 1b), compatible with the diagnosis of myotubular myopathy. Type 1 fiber predominance was remarkable (90%) (Fig. 1c). Genetic analysis of XLMTM revealed a splice-acceptor-site mutation of *MTM1* in intron 6 (c.445-1G>A), resulting in skipping of exon 7 at the cDNA level (Fig. 1d) [8]. The patient received respiratory support using non-invasive positive pressure ventilation, and underwent a tracheotomy at 8 months of age because of frequent asphyxia caused by aspiration.

At 5 years old, he was admitted to the Uwajima City Hospital for treatment of massive pneumonia and atelectasis in the left lung. Laboratory studies on admission showed that hemoglobin was 14.6 g/dL, white blood cell count was 11,400/μL, platelet count was 338,000/μL, aspartate aminotransferase was 69 IU/L, alkaline phosphatase was 73 IU/L, and C-reactive protein was 0.46 mg/dL. Bacterial blood and sputum cultures showed negative results. Fibrinolytic activity test on four days after admission remained within normal limits (prothorombin time was 11.9 s, fibrin degradation products was 8.6 μg/ml and D-dimer was 0.8 μg/ml). The patient gradually improved with a course of antibiotics (cefotaxime sodium) and lung physical therapy. Nine days after admission, a mechanically assisted coughing system was used as a mechanical in-exsufflator (MI-E) because of difficulty of sputum expectoration. The next day, he suffered from abrupt tachycardia and cyanosis. He had a peripheral coldness and his abdomen was gradually distended, especially the right costal margin, because of hepatic enlargement. Laboratory studies

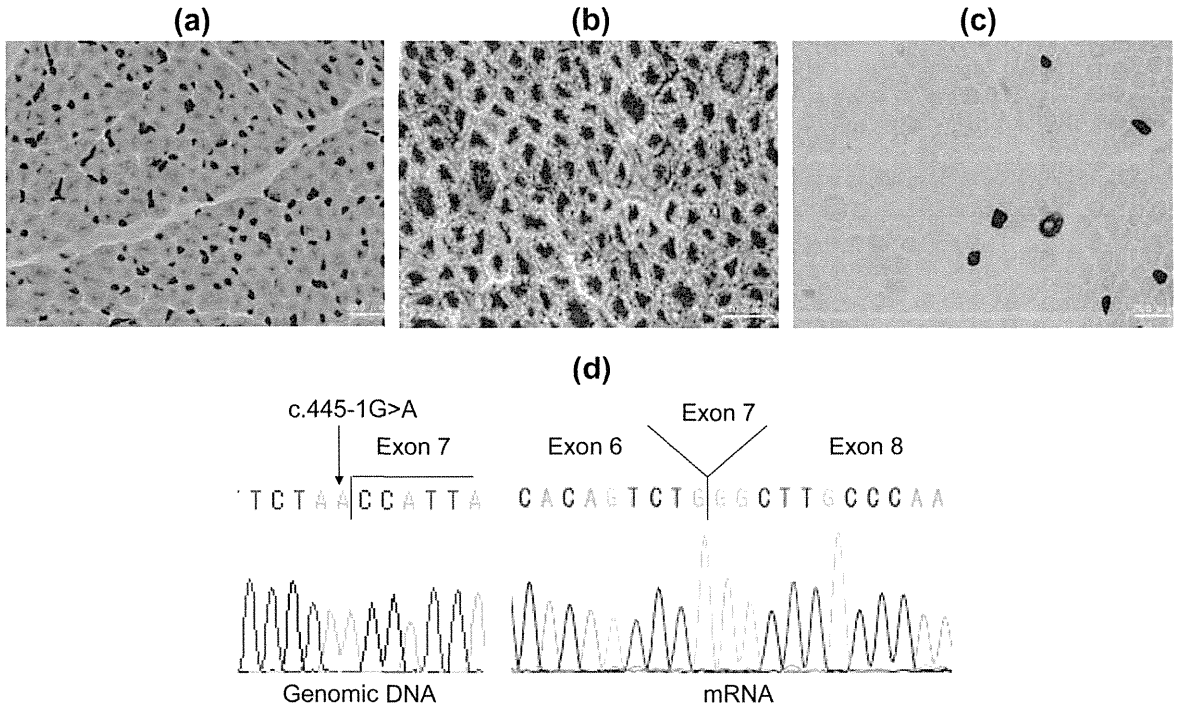


Fig. 1. Histological findings of muscle biopsy and genetic analysis. (a) Hematoxylin and eosin (H & E) staining shows that all muscle fibers are small and round. Marked perimysial fibrosis and scattered pyknotic nuclear clumps can be seen. Muscle fibers with central nuclei comprise 40% of the biopsy specimen. (b) As shown by nicotinamide adenine dinucleotide tetrazolium reductase staining, the intermyofibrillar network is markedly disorganized with peripheral halo features seen in most fibers. (c) On ATPase, types 1, 2A–C comprise 90%, 8%, 2%, and 0%, respectively. Type 2 fiber atrophy can be seen. (d) *MTM1* analysis revealed a splice-acceptor-site mutation in intron 6 (c.445-1G>A) at the genomic DNA level and skipping of exon 7 at the cDNA level.

Please cite this article in press as: Motoki T et al., Fatal hepatic hemorrhage by peliosis hepatis in X-linked myotubular myopathy: A case report, Neuromuscul Disord (2013), http://dx.doi.org/10.1016/j.nmd.2013.06.008

showed that the hemoglobin level and platelet count were decreased to 6.4 g/dL and 82,000/μL, respectively. An abdominal computed tomography (CT) scan showed hepatomegaly with a heterogeneous low density area expanding from the medial segment to the right lobe of the liver, and the leakage of contrast material into parenchyma during the arterial phase, suggesting the diagnosis of liver hemorrhage (Fig. 2a). There was little intraperitoneal bleeding. With rapid transfusion of red cells, a hepatic angiogram was performed via the common hepatic artery. Because active bleeding was observed within liver parenchyma (Fig. 2b), obstructing material (Gelpart® Molecular Devices, Nippon Kayaku Co. Ltd., Tokyo, Japan) was injected into the anterior and posterior branches of the hepatic artery to control active bleeding. Despite these treatments, hemoglobin levels gradually decreased from 11.1 to 3.8 g/dL 8 h after the obstruction therapy. The abdomen was further distended and pitting edema appeared in the lower body. Repeated abdominal CT showed massive intraperitoneal bleeding compared with that of the previous day, and a narrowed inferior vena cava caused by hepatic enlargement was detected. He died 4 days after the onset of acute hepatic hemorrhage. The autopsy indicated

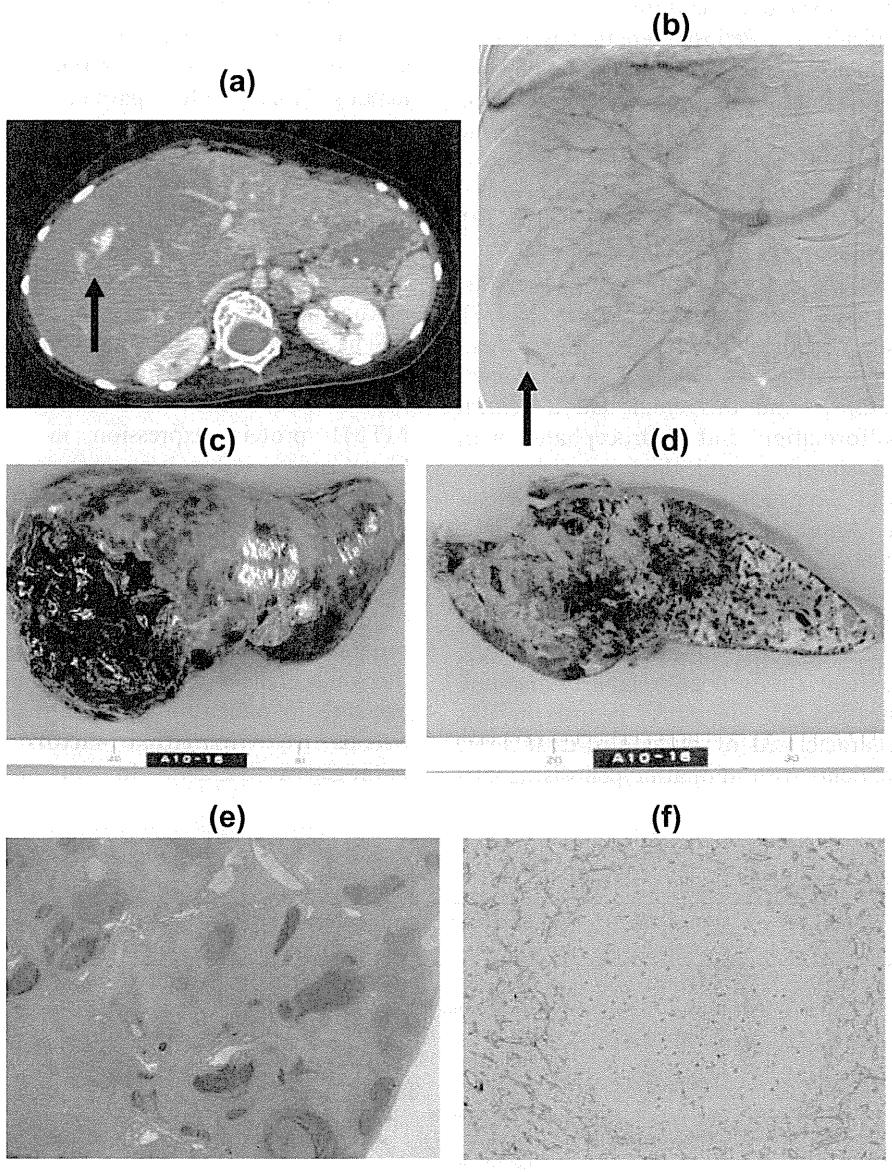


Fig. 2. Radiological and pathological findings of periosis hepatis. (a) Contrast abdominal CT shows hepatomegaly and a heterogeneous low density area extending from the medial segment to the right lobe of the liver. Contrast dye had leaked into the parenchyma (arrow) during the arterial phase. (b) A hepatic angiogram shows a number of retained contrast agents and some active bleeding (arrow) within liver parenchyma. (c and d) Autopsy findings show expansive intraperitoneal bleeding caused by rupture at the right hepatic capsule, and multiple variable-sized cystic blood-filled spaces were found in a section of the liver. (e) Multiple blood-filled spaces within the liver parenchyma can be seen (H & E). (f) Immunohistochemically, the inner surface of the blood-filled space is devoid of CD31-positive endothelial lining in contrast to the sinusoidal endothelia.

Please cite this article in press as: Motoki T et al., Fatal hepatic hemorrhage by peliosis hepatis in X-linked myotubular myopathy: A case report, Neuromuscul Disord (2013), http://dx.doi.org/10.1016/j.nmd.2013.06.008

expansive intraperitoneal bleeding caused by rupture of the right hepatic capsule (Fig. 2c). Multiple variable-sized cystic blood-filled spaces and hemorrhagic necrosis were found in the liver (Fig. 2d). Histopathologically, the liver contained multiple blood-filled spaces (Fig. 2e) that were devoid of CD31-positive endothelial lining (Fig. 2f), which was compatible with peliosis hepatis.

## 3. Discussion

Peliosis hepatis is a rare fatal disorder with a number of causes, and is defined as multiple, variable-sized, cystic, blood-filled spaces through the liver parenchyma, in which spaces are not covered by endothelium of blood vessels histopathologically [9]. Peliosis hepatis has mostly been reported in adult patients associated with chronic wasting disorder [10], human immunodeficiency virus infection [11–12], oral contraceptives [13], androgenic steroids [14], and *Bartonella henselae* infection [15], and is idiopathic [16]. In children, peliosis hepatis is rare and has only been reported with androgenic steroids [17–18], *Escherichia coli* pyelonephritis [19], and XLMTM [4–7].

In XLMTM, only six children with peliosis hepatis, including our case, have been reported (Table 1) [4–7], and five of them developed acute onset multiple organ failure. The remaining child was detected by chance at the time of the autopsy, and this child had a central nervous system malformation and hydrocephalus with ventriculo-peritoneal shunting, and died of a hypoxic episode at 4 years old. The mean age at onset of peliosis hepatis was 4 years. Antecedent infection before hepatic hemorrhage was observed in three patients, including our patient. An elevated liver function test was observed in three patients, including our patient, but was normal in two. Five of six patients died of acute fatal hepatic hemorrhage. One patient survived after laparotomy and transarterial embolization [5]. Therefore, peliosis hepatis with XLMTM is characterized by difficult-to-treat acute onset. Some adult patients with idiopathic peliosis hepatis have received successful emergent hepatectomy, liver transplantation, and arterial embolization [16,20]. However, once hepatic hemorrhage from peliosis hepatis occurs, it is usually difficult to control bleeding, as observed in our patient. Therefore, reducing the incidence and prompt recognition of hepatic hemorrhage are mandatory for XLMTM patients.

The diagnosis of peliosis hepatis is difficult and often missed or delayed because of the atypical findings on standard radiological tests. A previous report indicated that ultrasonic examination is useful to detect abnormal findings according to various liver conditions, and can show perinodular and intranodular vascularity in patients with peliosis hepatis [21]. Other imaging systems, including CT, magnetic resonance imaging, and angiography can also be helpful for diagnosis of peliosis hepatis [18,21]. Our patient showed persistent mild elevations in a serum liver function test before the episode of acute hemorrhage. He had not received a routine ultrasonic examination, and CT findings on admission indicated no hepatic lesion, suggesting hemorrhage or peliosis hepatis. Therefore, fatal hepatic hemorrhage from peliosis hepatis was induced by an unknown cause after admission.

The mechanism of peliosis hepatis remains to be fully elucidated. And the causal relationship between peliosis hepatis and XLMTM is poorly understood, although MTM1 protein expression in liver are reported in GeneCards®. It has been reported that a mechanical in-exsufflator (MI-E) is safe and effective for respiratory infections of pediatric patients with neuromuscular disorders [22]. MI-E was initially used for removing secretions in our case, and fatal hepatic hemorrhage occurred on the next day of MI-E adoption. In some reports describing the mechanism of peliosis hepatis, blockade of liver blood outflow and increased sinusoidal pressure in patients with abnormality of the sinusoidal barrier were important factors contributing to the pathogenesis [23,24]. In our case, there were no

Table 1
Summary of peliosis hepatis in XLMTM patients.

| No. | Age | Severity of XLMTM | Cognitive development | Detection of PH | Known liver dysfunction | Infection at the onset of PH | Diagnosis | Status |
|---|---|---|---|---|---|---|---|---|
| 1[4] | 5 y | Severe | Normal | Hepatic hemorrhage | Yes | Un-documented | Autospy | Deceased |
| 2[4] | 4 y | Severe | Normal | By chance (autospy) | No | Un-documented | Autospy | Deceased |
| 3[5] | 3 y | Severe/ moderate | Normal | Hepatic hemorrhage | No | URI otitis media | CT | Improved |
| 4[6] | 2 y 6 m | Severe | Un-documented | Hepatic hemorrhage | (Un-documented) | Un-documented | Autospy | Deceased |
| 5[7] | 5 y | Severe | Un-documented | Hepatic hemorrhage | Yes | Fever | Autospy | Deceased |
| 6 (present patient) | 5 y | Severe | Slightly retarded | Hepatic hemorrhage | Yes | Pneumonia | Autospy | Deceased |

PH: peliosis hepatis, URI: upper respiratory infection, CT: computed tomography.

Please cite this article in press as: Motoki T et al., Fatal hepatic hemorrhage by peliosis hepatis in X-linked myotubular myopathy: A case report, Neuromuscul Disord (2013), http://dx.doi.org/10.1016/j.nmd.2013.06.008